New metallicity calibration for Seyfert 2 galaxies based on the $N2O2$ index

C. S. Castro[1], O. L. Dors[1]⋆, M. V. Cardaci[2,3], G. F. Hägele[2,3]

[1] *Universidade do Vale do Paraíba, Av. Shishima Hifumi, 2911, Cep 12244-000, São José dos Campos, SP, Brazil*

[2] *Instituto de Astrofísica de La Plata (CONICET-UNLP), Argentina.*

[3] *Facultad de Ciencias Astronómicas y Geofísicas, Universidad Nacional de La Plata, Paseo del Bosque s/n, 1900 La Plata, Argentina.*

ABSTRACT

We derive a new relation between the metallicity of Seyfert 2 Active Galactic Nuclei (AGNs) and the intensity of the narrow emission-lines ratio $N2O2$=log([N II]λ6584/[O II]λ3727). The calibration of this relation was performed determining the metallicity (Z) of a sample of 58 AGNs through a diagram containing the observational data and the results of a grid of photoionization models obtained with the CLOUDY code. We find the new $Z/Z_\odot$-$N2O2$ relation using the obtained metallicity values and the corresponding observational emission line intensities for each object of the sample. Estimations derived through the use of this new calibration indicate that narrow line regions of Seyfert 2 galaxies exhibit a large range of metallicities ($0.3 \lesssim Z/Z_\odot \lesssim 2.0$), with a median value $Z \approx Z_\odot$. Regarding the possible existence of correlations between the luminosity $L(\text{H}\beta)$, the electron density, and the color excess E(B−V) with the metallicity in this kind of objects, we do not find correlations between them.

Key words: galaxies: general – galaxies: evolution – galaxies: abundances – galaxies: formation– galaxies: ISM

⋆ E-mail:olidors@univap.br

1   INTRODUCTION

Active Galactic Nuclei (AGNs) present in their spectra strong emission lines of heavy elements, easily measured even for objects at high redshifts. Therefore, the AGNs metallicities inferred through these emission-lines have an important role in the study of the chemical evolution of galaxies and of the Universe.

The metallicity of the gas phase of AGNs as well as of star-forming regions can be mainly obtained by two methods. The first one, generally called T_e-method, is based on measurements of emission-lines from the main ionization stages of a given element (e.g. O, N, S) and on direct measurements of the electron temperatures and densities of the gas (Osterbrock & Ferland 2006). The second one, called "strong-line method", uses a calibration between emission-line ratios easily measured and the metallicity or abundance of a given element, generally the oxygen (e.g. Pagel et al. 1979; Edmunds & Pagel 1984; Storchi-Bergmann et al. 1998; Pilyugin 2000, 2001; Kewley & Dopita 2002; Dors & Copetti 2005; Stasińska 2006; Maiolino et al. 2008; Berg et al. 2011; Dors et al. 2013; Brown et al. 2016; Pilyugin & Grebel 2016; Vale Asari et al. 2016). Concerning the applicability of the T_e-method, there is a consensus that it provides reliable metallicity estimations for star forming regions. In fact, Pilyugin (2003) showed that there is a good agreement (at least for the solar neighbourhood) between oxygen determinations based on the T_e-method and the ones derived through observations of the weak interstellar O Iλ1356 line towards the stars (see also Moss et al. 2002; Deharveng et al. 2000; Rolleston et al. 2000; Meyer et al. 1998). However, Dors et al. (2015) found that the T_e-method does not work for AGNs. These authors examined the relation between oxygen abundances (generally used as metallicity tracer) in the narrow-line regions (NLRs) of AGNs estimated from the T_e-method, strong-line method and through central intersect abundances in the host galaxies determined from the radial abundance gradients. They found that the T_e-method underestimates the expected oxygen abundances by until 0.8 dex and that this fact could be due to the presence of a secondary heating (ionizing) source in addition to the radiation produced in the inner parts of the AGN (see also Zhang et al. 2013; Prieto et al. 2005; Contini et al. 2012). Therefore, the strong-line method seems to be more reliable to be used in AGN metallicity determinations.

Along decades, several relations between strong emission-lines and oxygen abundances have been proposed for star-forming regions (see López-Sánchez & Esteban 2010, for a review). Despite metallicities of AGNs have been estimated by many authors (e.g. Feltre, Charlot & Gutkin

2016; Dors et al. 2015; Richardson et al. 2014; Batra & Baldwin 2014; Du et al. 2014; Wang et al. 2011; Dhanda et al. 2007; Baldwin et al. 2003; Hamann et al. 2002; Ferland et al. 1996; Hamann & Ferland 1993, 1992), it seems that the unique calibrations available in the literature are the ones proposed by Storchi-Bergmann et al. (1998) and by Dors et al. (2014), who used photoionization model results to obtain expressions easily applicable considering optical and ultraviolet emission lines, respectively.

With the above in mind, we use a grid of photoionization models to obtain a new relationship between abundances and the strong narrow emission-lines of Seyfert 2 (Sy2) AGNs observed in the optical spectral range. The present study is organized as follows. In Section 2 a description of the methodology used to obtain the index calibration is presented. In Sect. 3 the calibration obtained is presented. The discussion and the conclusions of the outcome are given in Sect. 4 and Sect. 5, respectively.

2 METHODOLOGY

To obtain a calibration of the relation between the metallicity and the strong emission-lines of Sy2 galaxies, we compiled intensities of narrow emission-lines from the literature. These observational data were compared with the results of a grid of photoionization models in order to estimate the metallicity of each object. In what follows, a description of the photoionization models and of the observational sample are presented.

2.1 Photoionization models

We build a grid of photoionization models using the version 13.0 of the CLOUDY code (Ferland et al. 2013). These models are similar to those used by Dors et al. (2014, 2012) and the reader is refereed to these works for a detailed description of them. In summary, for the Spectral Energy Distribution (SED) we considered two sources of continuum modelled by: a "Big Bump" component peaking at 1 Ryd with a high-energy and an infrared exponential cut-off, and a power law with an $\alpha_x = 1$ representing the X-ray source that dominates at high energies taking into account that its normalisation must provide an optical to X-ray spectral index $\alpha_{ox} = -1.4$. This α_{ox} value is the average of the observed values for the entire range of observed luminosities of AGNs by Miller et al. (2011) and Zamarani et al. (1981). Indeed, photoionization models assuming this SED are able to reproduce optical and infrared observational data of a large sample of AGNs (see Dors et al. 2012). In all

models, a fixed electron density (N_e) value of 500 cm^{-3} was assumed. It is a representative value for the NLRs densities in AGNs as showed by Dors et al. (2014). These authors also showed that Sy2 exhibits electron density values in the range $100 \lesssim N_e(\text{cm}^{-3}) \lesssim 2000$. Storchi-Bergmann et al. (1998) investigated the influence of the electron density on the [N II]$\lambda\lambda$6548,6584/Hα metallicity indicator, finding that it is suppressed by collisional de-excitation only for very high density values larger than their critical electron densities, e.g. $N_e \approx 10^5$ cm^{-3} (see also Zhang et al. 2004). For the [O II] emission lines λ3726 and λ3729, the critical density is in order of 2000 and 5000 cm^{-3}, respectively. Thus, effects of electron density on metallicity estimations based on [O II] lines could be relevant for some objects studied.

We computed a sequence of models with the logarithm of the ionization parameter ranging from $-4.0 \leq \log U \leq -1.0$, with a step of 0.5 dex. U is defined as $U = Q_{\text{ion}}/4\pi R_{\text{in}}^2 nc$, where Q_{ion} is the number of hydrogen ionizing photons emitted per second by the ionizing source, R_{in} is the distance from the ionization source to the inner surface of the ionized gas cloud (in cm), n is the particle density (in cm^{-3}), and c is the speed of light (Fergusonet al. 1997; Davidson 1977; Shields 1976; Mathews 1974). It is worth mentioning that models with different combination of Q_{ion}, R and n but that result in the same U are homologous models with the same predicted emission-line intensities (Bresolin et al. 1999).

The metallicity range considered was $0.5 \leqq Z/Z_\odot \leqq 4.0$. The abundance of all elements was linearly scaled to the solar metal composition[1], with the exception of the N abundance, which was taken from the following relation between N/O and O/H given by Dopita et al. (2000):

$$\begin{aligned} \log(\text{N/H}) &= -4.57 + \log(Z/Z_\odot); \text{ for } \log(Z/Z_\odot) \leqq -0.63, \\ \log(\text{N/H}) &= -3.94 + 2\,\log(Z/Z_\odot); \text{ otherwise.} \end{aligned} \quad (1)$$

Photoionization model grids assuming these ranges of U and $Z/Z_\odot$ values describe emission line intensities observed practically at all wavelengths (Nagao et al. 2002, 2006; Groves et al. 2006; Dors et al. 2012, 2014, 2015). Models assuming the presence of dust in the gas phase do not reproduce the majority of emission-line intensities of AGNs (Nagao et al. 2006; Matsuoka et al. 2009; Dors et al. 2014), hence all the considered models in this work were dust free.

---

[1] In the CLOUDY code (version 13.00) the solar oxygen abundance relative to hydrogen is adopted to be the one derived by Alende Prieto , Lambert & Asplund (2001), i.e. 12+log(O/H)=8.69.

2.2   Observational sample

Intensities of narrow emission lines of AGNs classified as Seyfert 2 and 1.9 (hereafter Sy2) observed in the optical range ($3000\,\text{Å} < \lambda < 7000\,\text{Å}$) were compiled from the literature. We did not consider AGNs classified as Seyfert 1 because these objects seem to have shock of gas with high velocity (300-500 km/s; Dopita 1995), which is not considered in the CLOUDY code. Observational data of LINERs were also not considered because the physics of these objects seems to be little understood and assumptions of standard photoionization models seem do not reproduce them (Storchi-Bergmann et al. 1998). Our selection criterion was the measurements of the intensities of the [O II]λ3727, [O III]λ5007, [N II]λ6584 and [S II]$\lambda\lambda$6716,6731 narrow emission-lines. Observational data of 47 Sy2 compiled by Dors et al. (2015) and 13 observed by Dopita et al. (2015) were considered. From this sample, only the objects that meet the criteria proposed by Kewley et al. (2001) to distinguish objects ionized by massive stars from those containing an active galactic nucleus (AGN) and/or gas shock were considered (see Fig. 1). Hence all objects with

$$\log[\text{O III}]\lambda 5007/\text{H}\beta \; > \; \frac{0.61}{[\log([\text{N II}]\lambda 6584/\text{H}\alpha)] - 0.47} + 1.19 \tag{2}$$

were selected. The final sample consists of 58 objects: 46 compiled by Dors et al. (2015) and 12 observed by Dopita et al. (2015). In Figure 1 the objects of our final sample and a curve representing the criterion defined by (Kewley et al. 2001) are shown. All objects have redshifts $z < 0.1$ and their emission line intensities were reddening corrected. Table 1 lists the identification, logarithm of the ionization parameter, metallicity, luminosity, electron density, color excess derived along the paper and the bibliographic reference for each object of the sample.

The objects compiled by Dors et al. (2015) were observed using long-slit spectroscopy and those from Dopita et al. (2015) were observed using integral-field spectroscopy, therefore, they constitute an heterogeneous sample, i.e. they were obtained using different observational techniques and measurement apertures. In Fig. 1 none segregation between the long-slit and integral-field data can be noted. The effects of using such data sample do not yield any bias on the abundance estimations (see a complete discussion about this point in Dors et al. 2013).

Table 1. Identification, ionization parameter and metallicity ($Z/Z_\odot$) estimated using *interpolation* from Fig. 3, $Z/Z_\odot$ through the *N2O2 index* (Eq. 4), $\log L(\mathrm{H}\beta)$, electron density (N_{e}), color excess E(B-V) and the original reference for the objects in our sample.

Identification	$\log U$	$Z/Z_\odot$		$\log L(\mathrm{H}\beta)(\mathrm{erg\ s^{-1}})$	N_{e} (cm^{-3})	E(B-V)	Reference
		Interpolation	N2O2				
IZw 92	-2.5	0.67	0.67	41.55	822.0	0.15	1
NGC 3393	-2.3	1.85	1.80	—	2022.0	0.20	1
Mrk 176	-2.5	1.22	1.12	40.02	535.0	0.60	1
3c033	-2.6	0.67	0.66	40.51	252.0	0.23	1
Mrk 3	-2.6	1.25	1.16	40.91	948.0	0.45	1
Mrk 573	-2.5	1.22	1.12	40.51	781.0	0.30	1
NGC 1068	-2.4	4.00	—	42.03	—	0.32	1
Mrk 78	-2.7	0.32	0.77	40.80	370.0	0.45	1
Mrk 34	-2.6	0.97	0.93	41.31	546.0	0.26	1
Mrk 1	-2.5	1.12	1.07	40.20	767.0	0.41	1
3c433	-3.0	1.02	1.10	40.36	50.0	0.57	1
Mrk 270	-2.9	0.87	0.82	39.72	1027.0	0.20	1
3c452	-3.0	1.00	1.02	40.17	50.0	0.47	1
Mrk 198	-2.8	1.22	1.16	40.34	111.0	0.22	1
Mrk 268	-3.0	1.17	1.46	40.69	260.0	0.40	1
Mrk 273	-3.2	0.67	0.62	40.25	50.0	0.86	1
NGC 3227	-2.7	1.62	1.62	—	647.0	0.36	1
Mrk 6	-2.5	1.09	1.01	—	647.0	0.37	1
ESO 138 G1	-2.5	0.57	0.59	—	685.0	0.29	1
NGC 5643	-2.7	0.87	0.82	40.59	141.0	0.52	1
NGC 1667	-3.2	0.92	0.90	39.06	281.0	1.31	1
Mrk 423	-3.2	0.82	0.75	40.13	239.0	0.35	1
Mrk 609	-2.7	1.50	1.55	40.54	239.0	0.57	1
Mrk 226SW	-3.1	0.75	0.69	—	296.0	0.53	1
NGC 3081	-2.6	1.32	1.29	—	693.0	0.33	1
NGC 3281	-2.7	1.32	1.30	—	974.0	0.56	1
NGC 3982	-2.5	1.00	0.95	—	819.0	0.24	1
NGC 4388	-2.5	0.92	0.83	—	343.0	0.39	1
NGC 5135	-2.8	1.30	1.36	—	492.0	0.56	1
NGC 5643	-2.7	0.92	0.89	40.59	451.0	0.56	1
NGC 5728	-2.7	1.30	1.30	41.10	606.0	0.54	1
NGC 6300	-2.9	0.77	0.73	—	360.0	0.70	1
NGC 6890	-2.3	1.75	1.61	—	176.0	0.27	1
IC 5063	-2.8	0.87	0.82	—	311.0	0.48	1
IC 5135	-2.9	1.07	1.09	—	471.0	0.55	1
Mrk 744	-2.6	1.62	1.59	39.88	606.0	—	1
Mrk 1066	-3.0	0.95	1.01	—-	—	—	1
NGC 5506	-2.7	1.19	1.15	39.68	809.0	0.68	1
NGC 2110	-3.1	1.07	1.12	39.68	395.0	0.53	1
NGC 3281	-2.8	0.92	0.90	39.22	471.0	0.68	1
Akn 347	-2.5	1.37	1.30	39.93	606.0	0.54	1
UM 16	-2.6	0.92	0.88	41.07	606.0	0.36	1
Mrk 533	-2.3	1.82	1.71	40.82	1046.0	0.35	1
IZw 92	-2.5	0.72	0.68	41.44	805.0	0.19	1
Mrk 612	-2.5	1.82	1.82	40.20	75.0	0.48	1
Mrk 622	-3.2	0.57	0.54	40.71	64.0	1.17	1
IC 1657	-2.5	0.85	0.81	39.24	40.0	—	2
IRAS 01475-0740	-3.0	1.25	1.20	39.80	90.0	—	2
IC 1816	-2.9	2.00	2.01	39.96	8691.0	—	2
NGC 1125	-2.8	1.00	0.97	39.70	403.0	—	2
MCG -06-23-038	-3.0	1.20	1.17	39.43	949.0	—	2
IRAS 11215-2806	-2.8	0.87	0.84	39.22	532.0	—	2
ESO 137-G34	-3.0	1.42	1.38	39.74	581.0	—	2
NGC 6300	-3.2	1.20	1.17	37.92	330.0	—	2
ESO103-G35	-2.7	1.25	1.23	39.35	2449.0	—	2
NGC 6926	-2.8	0.90	0.90	38.86	305.0	—	2
IC 1368	-2.7	0.95	1.02	38.78	217.0	—	2
NGC 7590	-2.7	0.97	1.00	38.54	121.0	—	2

References— (1) Data compiled by Dors et al. (2015). (2) Dopita et al. (2015).
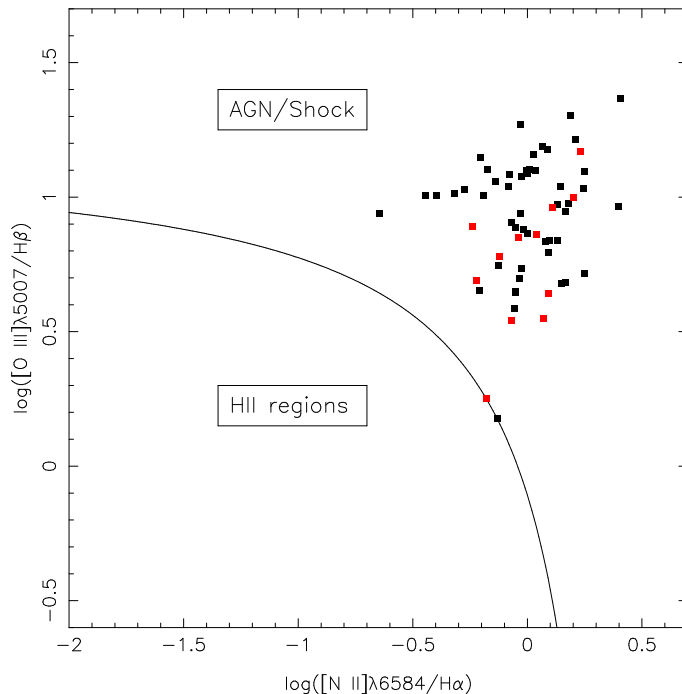
Figure 1. log[OIII]λ5007/Hβ vs. log([NII]λ6584/Hα) diagnostic diagram. Solid line, taken from Kewley et al. (2001), separates objects ionized by massive stars from those containing active nuclei and/or shock-excited gas (Equation 2). Black and red squares represent the objects taken from the compilation of Dors et al. (2015) and observed by Dopita et al. (2015), respectively, listed in Table 1.

3 $Z/Z_\odot$-$N2O2$ RELATION

The $N2O2$ index defined by

$$N2O2 = \log\left([\text{N II}]\lambda6584/[\text{O II}]\lambda3727\right) \tag{3}$$

was proposed by Dopita et al. (2000) to be applied in chemical abundance studies of star-forming objects (see also Kewley & Dopita 2002; Kewley & Ellison 2008). For star forming regions it has the advantage to be little dependent on the ionization parameter than other indexes (Kewley & Dopita 2002). To test if this result is also valid for Sy2s, predictions of our models for the $N2O2$ index and $N2$=log([N II]λ6584/Hα) versus the logarithm of the ionization parameter and for different metallicity values are shown in Fig. 2. The $N2$ index was proposed by Storchi-Bergmann et al. (1998) to be used as metallicity indicator of AGNs and it has also been applied in studies of star-forming regions (e.g. Pérez-Montero & Vílchez 2009). We can see that for each $Z/Z_\odot \leqq 2.0$ the $N2O2$ index ranges by about 0.5 dex for the entire $\log U$ range, while the $N2$ ranges by about 1 dex. For $Z/Z_\odot = 4.0$, a higher variation in both indexes is found. Moreover, we can note in Fig. 2 (top panel) that the $N2$ indicator does not show a monotonic behaviour with $Z/Z_\odot$.

The disadvantage of using strong-line metallicity relation based on the [N II] emission lines is the strong dependence of them on the N/O abundance ratio (Pérez-Montero & Vílchez
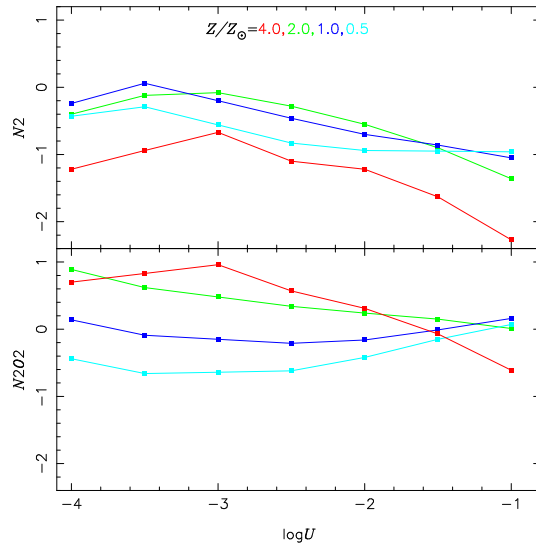
Figure 2. $N2O2 = \log([\text{NII}]\lambda6584/[\text{OII}]\lambda3727)$ and $N2 = \log([\text{NII}]\lambda6584/H\beta)$ versus the logarithm of the ionization parameter for different metallicities, lower and upper panel respectively. Lines connect predictions of our models (see Sect. 2.1) represented by points. Different colours represents our model results assuming different metallicities, as indicated.

2009), which is poorly known for AGNs. In fact, the majority of the photoionization model grids for AGNs has been built considering relations between N and O (or $Z/Z_\odot$) taken from metallicity studies of H II regions (e.g. Dors et al. 2015, 2014; Groves et al. 2006). For example, Storchi-Bergmann et al. (1998) assumed in their models a secondary origin for the nitrogen (N/O $\sim$ O/H) and they used a relation obtained for nuclear starbursts derived by Storchi-Bergmann et al. (1994). However, for the low metallicity regime ($Z \lesssim 0.3Z_\odot$), the nitrogen seems to have a primary origin (see e.g. Pilyugin, Thuan, & Vílchez 2003), which must be considered in AGNs models.

To calibrate the $N2O2$ index with the metallicity, we adopted the following method. We performed a [O III]$\lambda5007$/[O II]$\lambda3727$ versus [N II]$\lambda6584$/[O II]$\lambda3727$ diagram containing the results of our models (see Sect. 2.1) and the observational data (see Sect. 2.2). In Fig. 3 this diagram is shown. We can see that all observational data are located within the regions occupied by our models, with exception of one object, i.e. NGC 1068 (represented by a triangle in Fig. 3), not considered in our analysis.

In opposite to the model results of Storchi-Bergmann et al. (1998), it can be seen that the curves representing our photoionization model results overlap for the extreme $\log U$ values. Even though this method can not be used for these extreme values (i.e. $\log U \gtrsim -1.8$ and $\log U \lesssim -3.5$ for $Z/Z_\odot \gtrsim 2.0$) since we could not distinguish between two possible metallicity estimations, we can see from Fig. 3 that our observational data are located in a zone in which models do not overlap between them. Therefore, to calibrate the metallicity

as a function of the $N2O2$ index, we calculated the logarithm of the ionization parameter and the metallicity values for each object in our sample by linear interpolations between our models. These interpolated values are listed in the columns 2 and 3, respectively, of Table 1.

Among the objects selected, we found that NGC 7674 (not listed in Table 1) presents the highest measured metallicity value ($Z/Z_{\odot}$=3.35) in contrast to the relatively low value ($Z/Z_{\odot} \sim 0.5$) found by Dors et al. (2014) using their C43 index involving near-UV lines. Dors et al. (2015) also estimated low metallicity values for this object ($Z/Z_{\odot} \sim 1$) using the first calibration given by Storchi-Bergmann et al. (1998). The optical data of this object was originally published by Shuder & Osterbrock (1981), who reported the presence of blueward wings on all the emission lines used in the present work except on [O II]$\lambda 3727$. The observed difference in the shape of the emission lines could lead to underestimate the [O II]$\lambda 3727$ flux yielding a highest metallicity value. Hence, to prevent any possible bias introduced by NGC 7674 in the calibration we are going to perform, we take off NGC 7674 from our sample. The interpolated $Z/Z_{\odot}$ values together with the observational $N2O2$ values was considered and the following equation was obtained

$$(Z/Z_{\odot}) = 1.08(\pm 0.19) \times N2O2^2 + 1.78(\pm 0.07) \times N2O2 + 1.24(\pm 0.01). \tag{4}$$

In Fig. 4 the interpolated $Z/Z_{\odot}$ values as a function of $N2O2$ together with the fitted function are shown. Although this relation is unidimensional, i.e. it uses only one line ratio mainly dependent on the metallicity, it takes into account the dependence with the ionization parameter through the [O III]$\lambda 5007$/ [O II]$\lambda 3727$ ratio, which is strongly dependent on U, and that was considered in the $Z/Z_{\odot}$ estimations (see Fig. 3).

4 DISCUSSION

The metallicity of AGNs is an important parameter because it defines constraints for the regime of high metallicity in models of chemical evolution of galaxies (e.g. Cousin et al. 2016; Fu et al. 2013; Pilkington et al. 2012; Mollá & Díaz 2005) as well as it can be used to investigate the enrichment of the Universe (e.g. Dors et al. 2014; Matsuoka et al. 2009; Nagao et al. 2006).

Metallicity estimations of the NLRs of Sy2 galaxies and of the central regions of normal galaxies can be obtained, indirectly, by the use of the central intersect method (e.g. Dors et al. 2015; Gusev et al. 2012; Pilyugin, Thuan, & Vílchez 2007; Pilyugin et al. 2004;
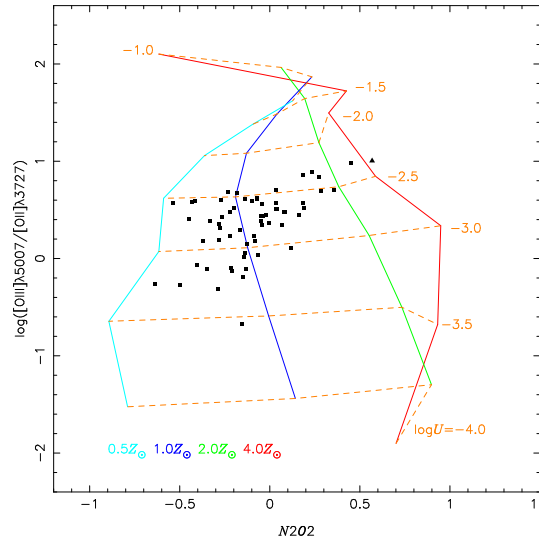
Figure 3. log([O III]λ5007/ [O II]λ3727) vs. $N2O2$ index. Solid lines connect our model results (see Sect. 2.1) of iso-metallicity, while the dashed lines connect curves of iso-ionization parameter, as indicated. Points represent the observational data compiled from the literature (see Sect. 2.2). The point out of the region occupied by the models (represented by a triangle) corresponds to NGC 1068.
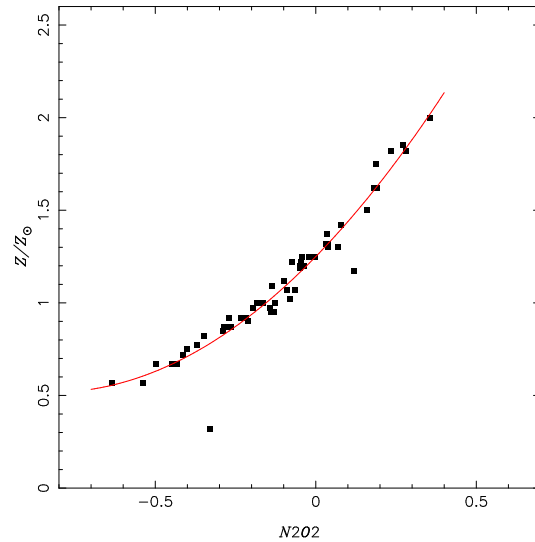

Figure 4. $Z/Z_\odot$ vs. $N2O2$ index. Points represent metallicity estimations obtained through our photoionization model results (see Sect. 3). Curve represents the fitting (see Eq. 4).

van Zee et al. 1998; Zaritsky et al. 1994; Vila-Costas & Edmunds 1992). This method consists in extrapolate to the central regions the radial abundance gradients of spiral galaxies estimated from spectroscopic data of H II regions located along their discs. Dors et al. (2015) found that abundances obtained by this method are similar or slightly higher than those obtained using strong line methods for a sample of objects for which there are direct spectral measurements. However, the central intersect method requires to observe a large sample of H II regions and it is limited to objects spatially resolved, i.e. objects with low redshifts. These authors also analysed the results obtained by the use of the T_e-method (which involve the weak auroral temperature sensitive emission-lines) finding that this method underesti-

mates the oxygen abundances by up to ~2 dex compared to the abundances derived through the strong-line method. Therefore, determinations based on strong emission-lines of AGNs seem the easiest and most reliable method.

Up to now, it seems that only three relationships between the metallicity or oxygen abundance and strong and narrow emission-lines of AGNs are available in the literature: the relationship based on ultraviolet emission lines proposed by Dors et al. (2014) and two relations based on optical emission-lines proposed by Storchi-Bergmann et al. (1998). Dors et al. (2015) showed that the first relationship proposed by Storchi-Bergmann et al. (1998), given by

$$
\begin{aligned}
(O/H)_{SB98,1} = {} & 8.34 + (0.212\,x) - (0.012\,x^2) - (0.002\,y) \\
& + (0.007\,xy) - (0.002\,x^2 y) + (6.52 \times 10^{-4}\,y^2) \\
& + (2.27 \times 10^{-4}\,xy^2) + (8.87 \times 10^{-5}\,x^2 y^2),
\end{aligned}
\tag{5}
$$

where $x = [\text{N\,{\footnotesize II}}]\lambda\lambda 6548{,}6584/\text{H}\alpha$ and $y = [\text{O\,{\footnotesize III}}]\lambda\lambda 4959{,}5007/\text{H}\beta$, presents a better agreement with recent photoionization models than the central intersect abundance method. Hereafter, we will compare this relation with our own (Eq. 4).

There are other line ratios that could be used as metallicity indicators of NLRs of Sy2 galaxies, e.g. the classical $R_{23} = ([\text{O\,II}]\lambda 3727 + [\text{O\,III}]\lambda 4959 + \lambda 5007)/\text{H}\beta$ empirical parameter suggested by Pagel et al. (1979) to estimate oxygen abundances in star-forming regions. Dors et al. (2015), using a grid of photoionization models, found a new O/H-R_{23} relation for NLRs of Sy2 galaxies. However, these authors pointed out that NLRs of Sy2 galaxies could have a secondary heating (ionizing) source –probably low-velocity shock gas– in addition to the radiation from the gas falling into the central engine, being the O/H-R_{23} relation not reliable for this kind of objects. The use of metallicity indicators based on strong emission-lines involving ions with similar ionization potential can minimize this effect. In this sense, the $N2O2$ index has advantage with respect to the majority of other metallicity indicators (see Kewley & Dopita 2002; López-Sánchez & Esteban 2010; Dors et al. 2011) because the involved ions, N^+ and O^+, have near ionization potentials, i.e. 29.60 eV and 35.12 eV, respectively.

With the aim to compare the metallicity estimated through our $N2O2$-$Z/Z_\odot$ relation with those obtained using the relation proposed by Storchi-Bergmann et al. (1998), we plotted in Fig. 5 both estimations for the objects in our sample (bottom panel) as well as the difference between them (top panel). The average difference between both estimations was
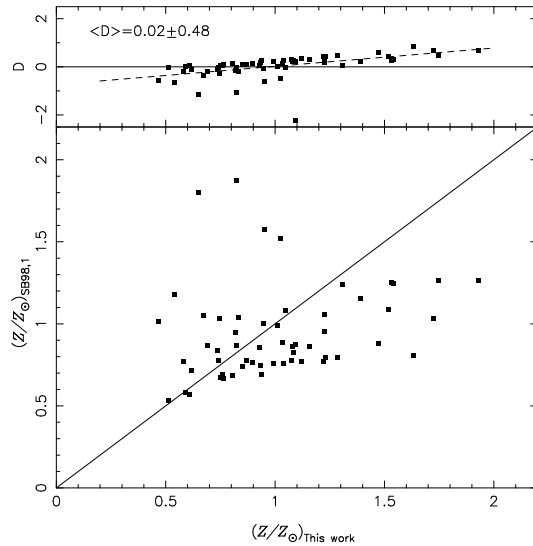
Figure 5. Bottom panel: Comparison between $Z/Z_\odot$ obtained using the calibrations proposed in this work and the one proposed by Storchi-Bergmann et al. (1998) for the objects in our sample. Top panel: Difference (D) between metallicity estimations based on our calibration (Eq. 4) and from the one proposed by Storchi-Bergmann et al. (1998), represented by Eq. 5. The average difference $\langle D \rangle$ between both estimations is indicated. Dashed line represents a linear regression to these differences, i.e. $D = 0.89(\pm 0.14) \times (Z/Z_\odot) - 0.86(\pm 0.17)$.

found to be $\langle D \rangle = 0.02 \pm 0.48$ and, based on the linear regression considering the estimations, it would seem that the calibration by Storchi-Bergmann et al. (1998) yields lower and higher values for the high and low metallicity regimes, respectively. However, the fact that most of the objects are located around $(Z/Z_\odot)=1$ could introduce a bias in the calculated linear regression coefficients (see upper panel of Fig. 5) due to the low numbers statistics in the extreme metallicity regimes. In order to investigate this discrepancy, the logarithm of the ionization parameter versus the difference between the estimations is shown in Fig. 6, where any correlation between can be seen. Therefore, the difference between metallicity estimations based on our calibration and those from the calibration proposed by Storchi-Bergmann et al. (1998) probably is due to the use of different N/O-O/H relations assumed in the models, the evolution of atomic parameters, inclusion of physical process in photoionization model codes or due to different methodology considered, hence Storchi-Bergmann et al. (1998) considered a theoretical calibration and we a semi-empirical one.

Analysing the metallicity distribution obtained applying our $N2O2$-$Z/Z_\odot$ relation to the objects in our sample (see histogram in Fig. 7), we found $\sim 55\%$ of the objects present metallicities in the $0.75 \leqq Z/Z_\odot \leqq 1.25$ range with a median value of ~ 1.00 (i.e. 12+log(O/H)=8.69, adopting the solar oxygen abundance to be $12 + \log(O/H)_\odot = 8.69$; Alende Prieto , Lambert & Asplund (2001)). The average value of the metallicity considering the whole sample is $< Z/Z_\odot >= 1.03(\pm 0.38)$, which corresponds to 12+log(O/H)=8.70(± 0.13).
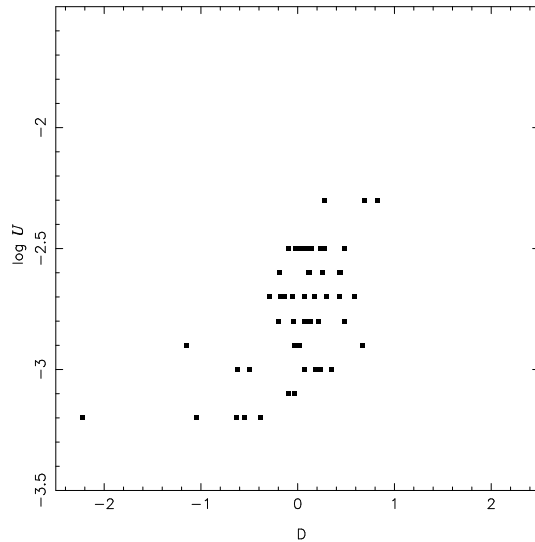
Figure 6. Logarithm of the ionization parameter (U) versus the difference (D) between metallicity estimations derived from our calibration (Eq. 4) and from the one proposed by Storchi-Bergmann et al. (1998), represented by Eq. 5. The log U and D were taken from Table 1 and Fig. 5, respectively.

Studying a large sample of star-forming regions, Pilyugin, Thuan, & Vílchez (2007, 2006) found, using the P-method (Pilyugin 2001, 2000), that there seems to be a maximum attainable oxygen abundance of 12+log(O/H)$\sim$ 8.87 ($Z/Z_\odot \sim 1.50$) for this kind of regions. Most of the objects in our sample show metallicity values lower than this maximum value derived for star-forming regions. We only found four objects (NGC 3393, Mrk 744, Mrk 533, IC 1816) with metallicity higher than the maximum estimated by Pilyugin and collaborators. Dors et al. (2015) also calculated the central oxygen abundance for a large sample of Sy2 active objects and star-forming nuclei of normal galaxies founding that most of the objects present metallicities in the range $0.6 \leqq Z/Z_\odot \leqq 2.0$, with few objects showing higher values. This is a similar result than the one derived in this work.

We investigated whether the metallicity is correlated or not with other Sy2 parameters. In first place, we analysed the correlation between the AGN luminosity and the metallicity for our sample of Sy2 objects. It is well known the existence of a strong correlation between the mass (or luminosity) and metallicity in ellipticals and spiral bulges (e.g. Faber et al. 1973, 1989; Zaritsky et al. 1994; Lequeux et al. 1979; Skillman et al. 1989; Garnett 2002; Pilyugin, Thuan, & Vílchez 2006), in the sense that the most metallic objects exhibit the highest mass (or luminosity) values. This relation seem to be due to action of galactic winds, in which massive objects have deeper gravitational potentials retaining their gas against the building thermal pressures from supernovae (see Hamann & Ferland 1999 and references therein). However, it is still barely known if a similar relation is followed by AGNs. In fact,
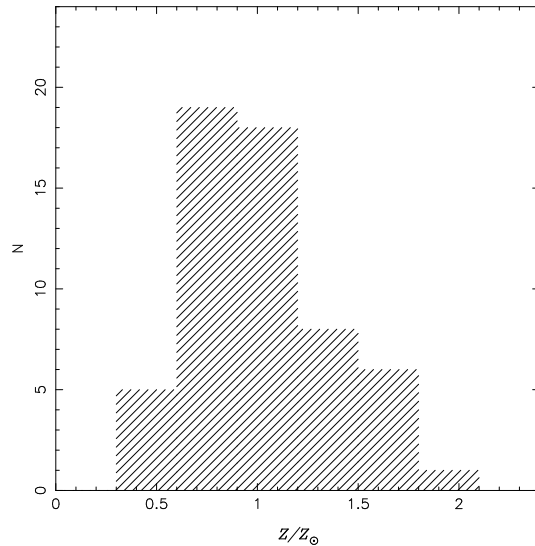
Figure 7. Histogram containing the metallicity values derived from the calibration between $N2O2$-$Z/Z_\odot$ (Eq. 4) for the sample of objects listed in Table 1.

Dors et al. (2014) and Nagao et al. (2006) found a slight increase of metallicity, calculated from UV emission lines, with the He II luminosity for a large sample of Sy2, Quasar and radio galaxy objects (see also Hamann & Ferland 1993, 1999). In order to verify if similar relation is obtained through our estimations, the luminosity of 46 of our objects were calculated using the published flux of Hβ, with the redshifts taken from NED[2] and assuming a spatially flat cosmology with $H_0 = 71\,\mathrm{km\,s^{-1}Mpc^{-1}}$, $\Omega_m = 0.270$, and $\Omega_{\mathrm{vac}} = 0.730$ (Wright 2006). These values are listed in the column 5 of Table 1. There are a large scatter in $L(\mathrm{H}\beta)$ for each value of $Z/Z_\odot$ (see bottom panel of Fig. 8), hence, any correlation was found.

We also investigated the behaviour of the electron density and of the internal dust content, traced by the color excess E(B-V), as a function of the metallicity for our sample of objects. In particular, the existence of correlations between these parameters are important in building models of accretion disk around black holes (e.g. Collin & Zahn 1999; Collin & Huré 1999) The electron density values (listed in the column 6 of Table 1) were estimated from the published [S II]$\lambda\lambda$6716,6731 emission-line intensities and using their relation with the electron density given by Dors et al. (2016). A large scatter was also found between the estimated densities and the metallicity (see middle panel of Fig. 8), hence, any correlation was found. Finally, we analysed the behaviour of the color excess E(B-V) derived from the nebular gas emission lines as defined by Jones et al. (2013) $\mathrm{E(B-V)} = 1.695 \log \frac{\mathrm{H}\alpha/\mathrm{H}\beta}{2.86}$

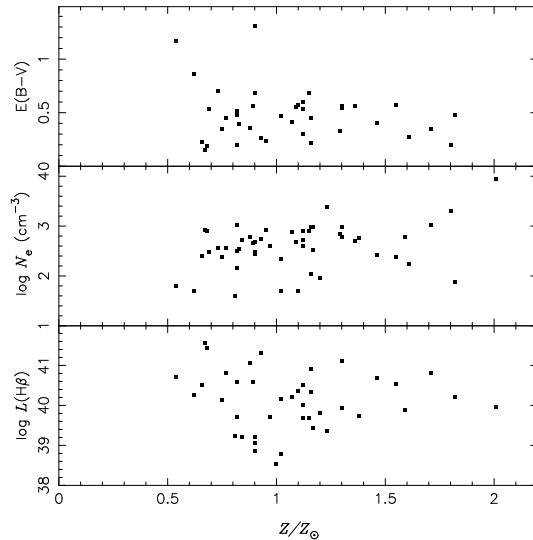**Figure 8.** $\log[L(\text{H}\beta)]$, $\log[N_e]$ and E(B-V) vs. $Z/Z_\odot$ (bottom, middle and top panel, respectively). Points represent estimations for the objects listed in Table 1.

(listed in the column 7 of Table 1) as a function of the metallicity (see top panel of Fig. 8). As in the previous cases we were not able to find any correlation between these parameters.

5   CONCLUSIONS

We proposed here a metallicity indicator for Sy2 AGNs based on the narrow emission line intensity ratio $N2O2=\log([\text{N\,\textsc{ii}}]\lambda6584/[\text{O\,\textsc{ii}}]\lambda3727)$. The calibration of the relation between $Z/Z_\odot$ and the $N2O2$ index was obtained using a sample of 58 Sy2 galaxies compiled from the literature for which we estimated their metallicities through a diagram containing the observational $\log([\text{O\,\textsc{iii}}]\lambda5007/[\text{O\,\textsc{ii}}]\lambda3727, N2O2$ ratios and the results of a grid of photoionization models obtained with the CLOUDY code. Using these estimated metallicity values together with the observational $N2O2$ index values estimated for the objects in our sample, we calibrated the $Z/Z_\odot$-$N2O2$ relation. Even though this relation depends on only one emission-line ratio, it also depends on the ionization parameter through the $[\text{O\,\textsc{iii}}]\lambda5007/[\text{O\,\textsc{ii}}]\lambda3727$ ratio used in the process to calibrate it. Using the calibration presented in this work, we found that Sy2 galaxies exhibit a large metallicity range ($0.3 \lesssim Z/Z_\odot \lesssim 2.0$), with a median value of $Z \approx Z_\odot$. Hence we did not find any extraordinary chemical enrichment in the narrow line regions of Sy2 AGNs. Likewise, any correlation was obtained between metallicity and the Hβ luminosity, the electron density, or the color excess E(B−V) for the objects in our sample.

ACKNOWLEDGMENTS

REFERENCES

Abazajian K. N. et al., 2009, ApJS, 182, 543

Alende Prieto C., Lambert D. L., Asplund M., 2001, ApJ, 556, L63

Baldwin J. A., Hamann F., Korista K. T., Ferland G. J., Dietrich M., Warner C., 2003, ApJ, 583, 649

Batra N. D., Baldwin J. A., 2014, MNRAS, 439. 771

Berg D. A., Skillman E. D., Marble A. R., 2011, ApJ, 738, 2

Bresolin F., Kennicutt R. C., Garnett D. R., 1999, ApJ, 510, 104

Brown J. S., Martini P., Andrews B. H., 2016, MNRAS, 458, 1529

Collin S., & Zahn J.-P., 1999, A&A, 344, 433

Collin S., & Huré J.-M., 1999, A&A, 341, 85

Contini M., 2012, MNRAS, 425, 1205

Cousin M., Buat V., Boissier S., Bethermin M., Roehlly Y., Génois M., 2016, A&A, 589, 109

Davidson K., 1977, ApJ, 218, 20

Deharveng L., Peňa M., Caplan J., Costero R., 2000, MNRAS, 311, 329

Dhanda N., Baldwin J. A., Bentz M. C., Osmer P. S., 2007, ApJ, 658, 804

Dopita M. A. et al., 2015, ApJS, 217, 12

Dopita M. A., Kewley L. J., Heisler C. A., Sutherland R. S., 2000, ApJ., 542, 224

Dopita M. A., 1995, Ap&SS, 233, 215

Dors O. L., & Copetti M. V. F., 2005, A&A, 437, 837

Dors O. L., Krabbe A. C., Hägele G. F., Pérez-Montero E., 2011, MNRAS, 415, 3616

Dors O. L., Riffel R. A., Cardaci M. V., Hägele G. F., Krabbe A. C., Pérez-Montero E., Rodrigues I., 2012, MNRAS, 422, 252

Dors O. L., et al., 2013, MNRAS, 432, 2512

Dors O. L., Cardaci M. V., Hägele G. F., Krabbe Â. C., 2014, MNRAS, 443, 1291

Dors O. L., Cardaci M. V., Hägele G. F., Rodrigues I., Grebel E. K., Pilyugin, L. S., Freitas-Lemes, P., Krabbe Â. C., 2015, MNRAS, 453, 4102

Dors O. L.,Pérez-Montero E., Hägele G. F., Cardaci M. V., Krabbe A. C., 2016, MNRAS, 456, 4407

Du P. et al., 2014, MNRAS, 438, 2828

Edmunds M. G., & Pagel B. E. J. 1984, MNRAS, 211, 507

Faber S. M., 1973, ApJ, 179, 423

Faber S. M. et al., 1989, ApJSS, 69, 763

Feltre A., Charlot S., Gutkin J., 2016, MNRAS, 456, 3354

Ferguson J. W., Korista K. T., Baldwin J. A., Ferland G. J., ApJ, 1997, 487, 122

Ferland G. J., 2013, Rev. Mex. Astron. Astrofis., 49, 137

Ferland G. J. et al. 1996, ApJ, 461, 683

Fu J. et al., 2013, MNRAS, 434, 1531

Garnett D. R. 2002, ApJ, 581, 1019

Groves B. A., Heckman T. M., Kauffmann G., 2006, MNRAS, 371, 1559

Gusev A. S., Pilyugin L. S., Sakhibov F., Dodonov S. N., Ezhkova O. V., Khramtsova M. S., 2012, MNRAS, 424, 1930

Hamann F., & Ferland G. J., 1992, ApJ, 391, 53

Hamann F., & Ferland G. J., 1993, ApJ, 418, 11

Hamann, F., & Ferland, G. J. 1999, ARA&A, 37, 487

Hamann F., Korista K. T., Ferland G. J., Warner C., Baldwin J., 2002, ApJ, 564, 592

Jones T., Ellis R. S., Richard S., Schenker M. A., Stark D. P., 2013, ApJ, 765, 48

Kewley L. J., Dopita M. A., Sutherland R. S., Heisler C. A., Trevena J., 2001, ApJ, 556, 121

Kewley L. J., Dopita M. A., 2002, ApJS, 142, 35

Kewley L. J., Ellison, S. L., 2008, ApJ, 681, 1183

López-Sánchez A. R., & Esteban C., 2010, A&A, 517, 85

Lequeux J., Rayo J. F., Serrano A., Peimbert M., Torres-Peimbert S., 1979, A&A, 80, 155

Maiolino R. et al., 2008, A&A, 488, 463

Mathews W. G., 1974, ApJ, 189, 23

Matsuoka K., Nagao T., Maiolino R., Marconi A., Taniguchi Y., 2009, A&A, 503, 721

Meyer D. M., Jura M., Cardelli J. A., 1998, ApJ, 493, 222

Miller B. P., BrandtW. N., Schneider D. P., Gibson R. R., Steffen A. T.,Wu J., 2011, ApJ,

726, 20

Mollá M., & Díaz A. I., 2005, MNRAS, 358, 521

Moos H. W. et al., 2002, ApJS, 140, 3

Nagao T., Murayama T., Shioya Y., Taniguchi Y., 2002, ApJ, 575, 721

Nagao T., Maiolino R., Marconi A., 2006, A&A, 447, 863

Osterbrock D. E., Ferland G., 2006, Astrophysics of Gaseous Nebulae and Active Galactic
Nuclei. -2nd ed. Unviersity Science Books, Mill Valley, CA

Pagel B. E. J., Edmunds M. G., Blackwell D. E., Chun M. S., Smith G., 1979, MNRAS,
189, 95

Pérez-Montero, E., & Vílchez, J.M., 2009, MNRAS, 400, 1721

Pilkington K. et al., 2012, A&A, 540, 56

Pilyugin L. S., 2000, A&A, 362, 325

Pilyugin L. S., 2001, A&A, 369, 594

Pilyugin L. S., 2003, A&A, 399, 1003

Pilyugin L. S., Thuan T. X., Vílchez J. M., 2003, A&A, 397, 487

Pilyugin L. S., Thuan T. X., Vílchez J. M., 2006, MNRAS, 367, 1139

Pilyugin L. S., Thuan T. X., Vílchez J. M., 2007, MNRAS, 376, 353

Pilyugin L. S., Vílchez J. M., Contini T., 2004, A&A, 425, 849

Pilyugin L. S. & Grebel E. K., 2016, MNRAS, 457, 3678

Prieto M. A., Marco, O., Gallimore, J., 2005, MNRAS, 364, L28

Richardson C. T., Allen J. T., Baldwin J. A., Hewett P. C., Ferland G. J., 2014, MNRAS,
437, 2376

Rolleston W. R. J., Smartt S. J., Dufton P. L., Ryans R. S. I., 2000, A&A, 363, 537

Shields G. A., 1976, ApJ, 204, 330

Skillman E. D., Kennicutt R. C., Hodge P. W. 1989, ApJ, 347, 875

Stasińska G., 2006, A&A, 454L, 127

Storchi-Bergmann T., Schmitt H. R., Calzetti D., Kinney A. L., 1998, AJ, 115, 909

Storchi-Bergmann T., Calzetti, D., Kinney, A. L. 1994, ApJ, 429, 572

Shuder J. M., & Osterbrock D. E., 1981, ApJ, 250, 55

Vale Asari N., Stasińska G., Morisset C., Cid Fernandes R., 2016, MNRAS, 460, 1739

van Zee L., Salzer J. J., Haynes M. P., O'Donoghue A. A., Balonek T. J., 1998, AJ, 116,
2805

Vila-Costas M. B., Edmunds M. G., 1992, MNRAS, 259, 121

Wang J. M. et al., 2011, ApJ, 739, 3

Wright E. L. 2006, PASP, 118, 1711

Zamorani G. et al., 1981, ApJ, 245, 357

Zaritsky D., Kennicutt R. C., Huchra, J. P., 1994, ApJ, 420, 87

Zhang Z. T., Liang Y. C., Hammer F., 2013, MNRAS, 430, 2605

Zhang Y. et al., 2004, MNRAS, 351